Journal of Power Sources, 29 (1990) 565 - 577

ADVANCED HIGH-TEMPERATURE BATTERIES

P. A. NELSON
Argonne National Laboratory, Argonne, IL 60439 (U.S.A.)

Summary

Recent results for Li–Al/FeS_2 cells and a bipolar battery design have shown the possibility of achieving high specific energy (210 W h kg^{-1}) and high specific power (239 W kg^{-1}) at the cell level for an electric vehicle application. Outstanding performance is also projected for sodium/metal chloride cells having large electrolyte areas and thin, positive electrodes.

Introduction

Work has been under way for about two decades on high-temperature batteries having lithium or sodium negative electrodes. These efforts have met with some success, but the original promise of very high specific energy and power has not been achieved for practical battery systems. This paper discusses some recent new approaches to achieving high performance for lithium/FeS_2 cells and sodium/metal chloride cells.

A comparison of the voltages and theoretical specific energies for several high-temperature cell couples is shown in Table 1. The fraction of the theoretical specific energy that can be achieved for practical cells differs markedly among the couples shown in the Table. The important factors in determining that fraction are the voltages of the cells and the densities of the reactants and the discharge products. The densities of the materials have a surprisingly important effect on the achievable specific energy, as is discussed in more detail below.

Lithium/disulfide batteries

The main problems for the development of successful Li–Al/FeS_2 cells have been (i) instability of the FeS_2 electrode, which has resulted in rapidly declining capacity; (ii) the lack of an internal mechanism for accommodating overcharge of a cell, thus requiring the use of external charge control on each individual cell; (iii) the lack of a suitable current collector for the positive electrode other than expensive molybdenum sheet material. Much progress has been made an ANL in solving the first two problems, and a new approach to cell design may result in a solution for the materials problem.

0378-7753/90/$3.50

TABLE 1

Comparison of high-temperature cell couples

System	Positive electrode discharge product	Average open circuit voltage (V)	Theoretical specific energy, (W h kg^{-1})
Li–Al/FeS	Li_2S, Fe	1.34	460
Li–Al/FeS_2	Li_2FeS_2	1.67	475
Li–Al/FeS_2	Li_2S, Fe	1.50	630
Na/$FeCl_2$	NaCl, Fe	2.35	728
Na/$NiCl_2$	NaCl, Ni	2.59	794
Na/S	Na–$S_{1.5}$	2.01	760

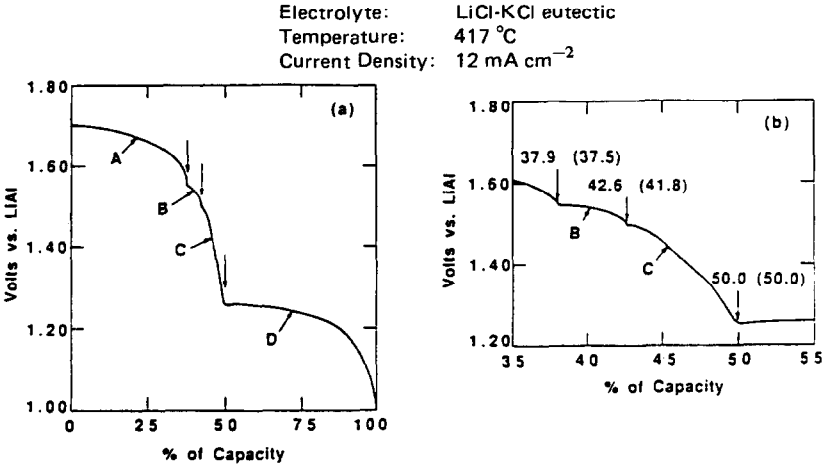

$$FeS_2 \xrightarrow{A} Li_3Fe_2S_4 \xrightarrow{B} Li_{2-x}Fe_{1-x}S_2 + Fe_{1-x}S \xrightarrow{C} Li_2FeS_2 \xrightarrow{D} Li_2S + Fe$$

Fig. 1. Discharge curve for LiAl/FeS_2 cell. Electrolyte, LiCl–KCl eutectic; temperature, 417 °C; current density, 12 mA cm^{-2}.

The disulfide electrode discharges along two major voltage plateaux, as shown in Fig. 1 [1]. It has been found practical to limit the amount of lithium in the negative electrode to stop the discharge at the end of the first major plateau, with a final discharge product of Li_2FeS_2. Although this limits the theoretical specific energy to about 475 W h kg^{-1} (second row, Table 1, based on Li–50 at.% Al), the positive electrode can be fabricated as a much denser electrode without provision for the large volume of Li_2S produced in operating on the lower voltage plateau.

The early problem on the stability of the FeS_2 electrode involved the disassociation of FeS_2 at high voltages on charge with the formation of

polysulfide ions, which dissolve in the electrolyte and then result in deposition of lithium sulfide in the separator region.

Kaun, at Argonne National Laboratory, studied this stability problem and also sought to achieve higher energy and power by the incorporation of dense FeS_2 electrodes operated only on the upper voltage plateau [2, 3]. He found that the use of dense FeS_2 electrodes not only improves the specific energy, but also improves the electrode conductivity and results in higher power. In most of the earlier work, the electrolyte was the LiCl–KCl eutectic (m.p., 352 °C), which required operation of the cell at about 450 °C because of polarization of the electrolyte, with high composition gradients at high operating rates. Kaun introduced the use of an LiCl–LiBr–KBr electrolyte, having a lower melting point and a broader liquidus range than those of the LiCl–KCl electrolyte, permitting operation at 400 °C. The combination of these changes improved the electrode utilization by 50% and doubled the power capability of the electrode at 80% depth-of-discharge (Fig. 2). These changes also resulted in a dramatic improvement in cycle life capability, as shown in Fig. 3.

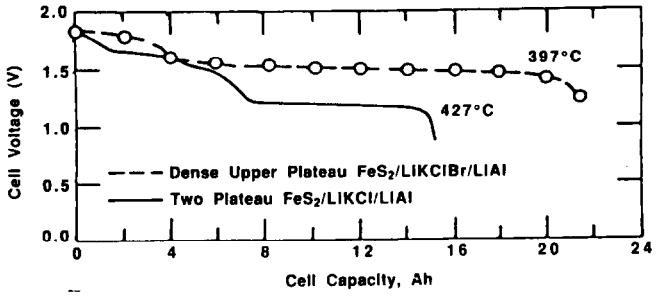

Fig. 2. Voltage *vs.* capacity for two types of disulfide electrodes having 24 A h loadings.

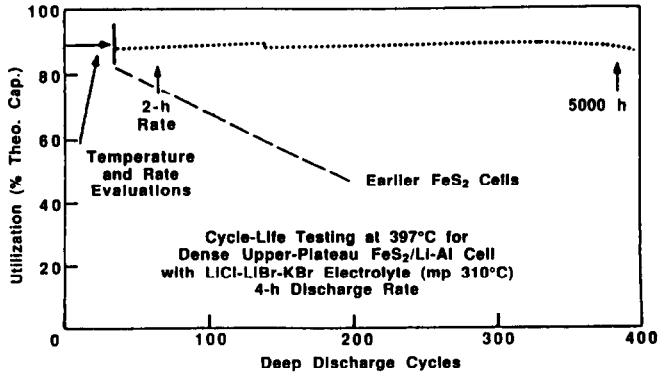

Fig. 3. Cycle life testing of dense upper-plateau of FeS_2 cell.

Another key improvement has been the development of a chemical overcharge protection mechanism [4]. By providing an excess of lithium relative to the aluminum or other alloy elements, a high lithium activity at the negative electrode is reached at the end of charge. This results in an increase in the dissolved lithium concentration in the electrolyte as the cell approaches full charge and, thus, about a twentyfold increase in the rate of self-discharge for the cell. By maintaining a low trickle-charge rate for several hours at the end of the charge, cells that are only partially charged have an opportunity to come to full charge, while fully charged cells tolerate the overcharging by the increase in the self-discharge rate.

Recently, work has begun on bipolar Li–Al/FeS_2 cells. The bipolar configuration reduces the amount of nonactive material required in the cell, and it provides a simpler design for the use of a coated material to reduce the cost of the disulfide electrode current collector. A schematic of the experimental cells now under development is shown in Fig. 4.

Researchers at ANL have used the results of cell tests to project the performance of Li–Al/FeS and Li–Al/FeS_2 cells in both the bicell and bipolar configuration. The results are summarized in Table 2. The capacity and power at the end of discharge (EOD) of the four types of lithium/sulfide cells in the Table were selected to be appropriate for the Eaton DSEP van being developed by Chrysler and Eaton in a program for the Electric and Hybrid Propulsion Division of the Department of Energy. The specific energy of the multiplate monosulfide cell is essentially that which has been already achieved in the laboratory, but the specific power assumes about a 50% improvement, which is expected to be achieved with thinner electrodes. The bipolar monosulfide calculations are based on the electrode performances used for the multiplate cells, with the weight of the cell calculated by adding the weight of individual parts. The bipolar monosulfide cell would be approximately 7.5 in. in diameter and have electrodes 7 in. in diameter. The performance of the disulfide bicell is based on results achieved in the laboratory for smaller cells, with the weight calculated from the individual components. The calculations for the disulfide bipolar cell were based on the monosulfide bipolar calculations, with substitution of parts as necessary for the disulfide conditions.

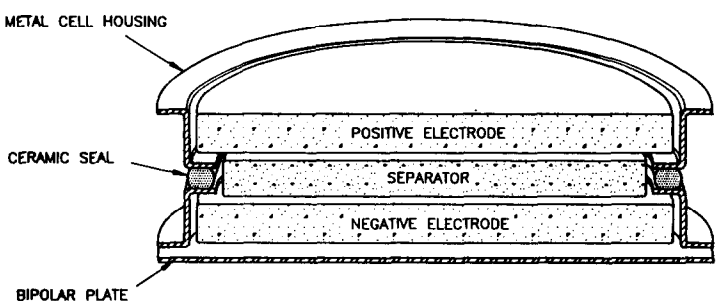

Fig. 4. Bipolar lithium/iron sulfide cell concept.

TABLE 2

Lithium/sulfide cells — Projected performance
Based on Eaton DSEP Van requirements

Characteristic	Monosulfide multiplate	Monosulfide bipolar	Disulfide bicell	Disulfide bipolar
Capacity (A h)	313	92	137	87
Specific energy (W h kg^{-1})	112	160	175	210
Specific power at EOD (W kg^{-1})	127	182	199	239
Weight (g)	3410	686	1250	663
Volume (cm^3)	1310	250	455	240

TABLE 3

Lithium/sulfide van batteries — projected performance

Basis: Eaton DSEP Van. Vehicle weight: Base, 1376 kg; load, 273 kg; total, 1649 kg + battery weight.
Range: 125 miles (range at end of battery life: 100 miles).
Energy usage: 0.194 W h (tonne mile)$^{-1}$ (FUDS cycle).
Power requirement (end of discharge, end of battery life): 23 kW $tonne^{-1}$ (0 - 50 mph/20 s).
Electronic control: 400 A max., 200 V max. open-circuit voltage.

Characteristic	Monosulfide multiplate	Monosulfide bipolar	Disulfide bicell	Disulfide bipolar
Cells per battery	150	450	224	336
Number of parallel strings	1	3	2	3
Capacity (FUDS cycle) (kW h)	56.4	49.4	49.0	46.8
Power at EOD (kW)[a]	64	56.3	55.7	53.3
Specific energy (W h kg^{-1})	83	127	132	167
Specific power (W kg^{-1})	94	144	151	190
Weight (kg)	680	390	370	280
Cell fraction of battery wt.	0.75	0.80	0.75	0.80
Volume (l)	415	227	225	163
Dimensions (in.)	59 L x 43 W x 10 H	59 L x 10 D (3)[b]	42 L x 33 W x 10 H	42 L x 10 D (3)[b]
Rate of heat loss (W)	300	200	200	200

[a]20% additional power over requirement is provided for new batteries to allow for battery degradation.
[b]Dimension shown are for each of three modules.

Table 3 gives the projected performance for batteries constructed for the Eaton DSEP van. These results are based on the projected cell performances of Table 2. The initial range of the vehicle with a new battery would be 125 miles. At the end of battery life it would be 100 miles. The energy storage required of the battery was adjusted for the total weight of the vehicle, including the battery, to achieve the desired vehicle range (Table 3). It should be noted that the vehicle weight is a function of the battery

weight, being 1649 kg plus the battery weight. The power at the end of discharge and at the end of battery life is sufficient to accelerate the vehicle to 50 mph in 20 s. With new batteries, for which the powers at the end of battery discharge are given in the Table, the acceleration would be approximately 20% more rapid than at the end of life.

The number of parallel strings in the batteries varies from one for the monosulfide multiplate to three for the bipolar batteries. For the bipolar batteries, each string would be housed in a separate insulating container of approximately 10 in. o.d.

Tests of very thin Li–Al/FeS_2 cells are appropriate for pulsed power applications. Figure 5 shows the apparatus used by Redey [5] for a pulsed discharge measurement, and Fig. 6 shows the results that were achieved in a discharge of approximately one millisecond. The calculated results show a specific power of 82.7 kW kg^{-1} and a power-to-energy ratio of 574 W $(W\ h)^{-1}$ (Table 4).

Sodium/metal chloride batteries

Sodium/sulfur batteries and sodium/metal chloride batteries have demonstrated good reliability and long cycle life. For applications where very high power is desired, new electrolyte configurations would be required.

The sodium/metal chloride cells are related to sodium/sulfur cells in that they both use molten sodium negative electrodes and a β''-alumina solid electrolyte. The sodium/metal chloride system was invented in South Africa and is now being developed under the direction of Anglo America of South Africa. The principal organizations involved in this development effort include Harwell and Beta Research and Development Ltd. of England, and Zebra Power Systems of South Africa.

The sodium/metal chloride cells, unlike the sodium/sulfur cells, utilize a secondary, liquid NaCl–$AlCl_3$ electrolyte in the positive electrode in conjunction with an active material of metal chloride, such as $FeCl_2$ or $NiCl_2$ [6 - 16]. Because the NaCl and the metal chloride are insoluble in NaCl–$AlCl_4$ at the operating conditions, the NaCl–$AlCl_3$ electrolyte acts only to transfer sodium ions within the positive electrode. The cells can be operated at temperatures down to 160 °C (the melting point of the liquid electrolyte), but are typically operated in present development work at 250 °C to improve the kinetics of the positive electrodes.

The voltages and theoretical specific energies are given in Table 1, and the overall reactions for the Na/$FeCl_2$ and Na/$NiCl_2$ cells are shown below:

$$2Na + FeCl_2 \Longleftrightarrow 2NaCl + Fe$$

$$2Na + NiCl_2 \Longleftrightarrow 2NaCl + Ni$$

An important feature of the metal chloride cells is that they are commonly fabricated in the uncharged state. For the Na/$FeCl_2$ cell, iron powder is

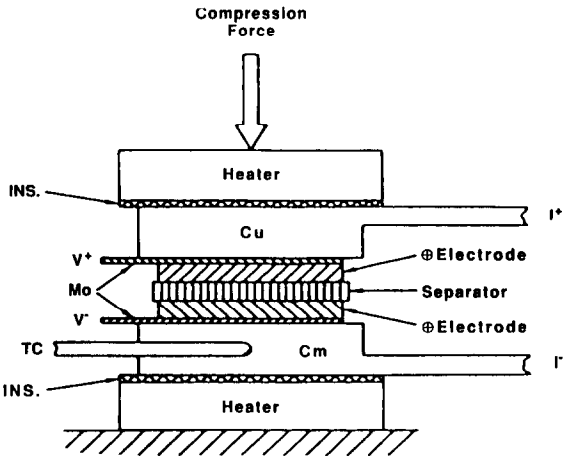

Fig. 5. Apparatus for pulsed discharge measurements on Li–Alloy/FeS_2 cells.

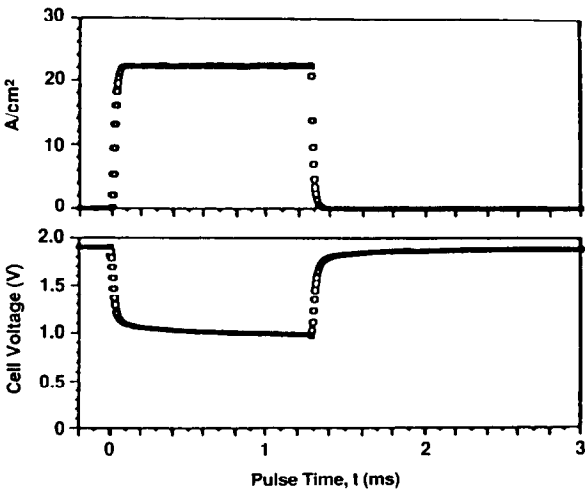

Fig. 6. Current density and voltage for 1 mS power pulse for Li–Al/FeS_2 cell achieving 24.1 W cm^{-2} at 490 °C. Sampling interval is 5 μs.

mixed with NaCl powder and pressed into a positive electrode. The NaCl–$AlCl_3$ electrolyte is added to the top of the positive electrode material as a dry powder, and the cell is charged after heating to the operating temperature. An important feature of fabricating the Na/MCl_2 cells in the uncharged state is that the reactants are relatively inexpensive and easily purified. The iron powder required for the Na/$FeCl_2$ cell is considerably less expensive than the nickel powder required for the Na/$NiCl_2$ cell, an obvious cost advantage, but the Na/$NiCl_2$ cell has better potential performance.

TABLE 4

Design and performance data for Li–Al/FeS_2 cell discharge for 1 ms at 440 °C

Components	
Positive electrode	FeS_2
Separator	BN + MgO
Electrolyte	LiF–LiCl–LiBr
Negative electrode	Li–Al
Bipolar plate	Mo
Design parameters	
Mass (g cm^{-2})	0.292
Thickness (cm)	0.123
Area loading (mA h cm^{-2})	42
Electrolyte condition	flooded
Performance parameters	
Measured	
Area specific impedance (mΩ cm^2)	41
Area specific power (W cm^{-2})	24.1
Derived	
Specific energy (W h kg^{-1})	144
Specific power (kW h kg^{-1})	82.7
Power density (kW l^{-1})	196
Power to energy (W (W h)$^{-1}$)	574

Most of the work on $Na/FeCl_2$ and $Na/NiCl_2$ cells described in the published literature [6, 7] has been on cells of 100 A h, or even larger, capacity. Batteries of such cells are already being tested in electric vehicles and appear to be rugged and reliable. This reliability results from connecting the cells into a single series-connected string. Unlike Na/S cells, Na/MCl_2 cells usually fail in the closed-circuit condition. Large Na/MCl_2 cells can be connected in series, with the loss of a cell resulting only in the loss of voltage associated with that cell and, essentially, no less of ampere-hour capacity for the entire battery.

The consequence of fabricating such large cells with a single β-alumina electrolyte tube is that the cells have only moderate power and large voltage drops when discharged at the 3-h rate. Also, to achieve even moderate discharge rates for the thick positive electrodes requires a high volume fraction of molten salt electrolyte. This adds to the weight and, coupled with the large reduction in voltage from that of an open circuit, results in achieving a low fraction of the theoretical specific energy. As an example, $Na/NiCl_2$ battery cells of 100 A h capacity were reported to achieve a specific energy of about 109 W h kg^{-1} and have a cell resistance of 9 mΩ [8]. When these cells were operated in a 66-cell battery, the energy was reduced to 88 W h kg^{-1} and 95 W h l^{-1}, which are less than the desired values for an advanced battery. However, the small reduction in specific energy of the battery compared with that of the cells is encouraging and results from the high density

and high packing density of the cells. The life of both the cells and the batteries is reported to be excellent (<1000 cycles).

An important feature of the Na/MCl_2 cell is that, in the positive electrode, the MCl_2 material is in thermodynamic equilibrium with the metallic constituent (iron or nickel) and does not appear to attack current collector materials made of the same metal. By contrast, polysulfides in the positive electrode of sodium/sulfur cells tend to attack most metals and alloys except, perhaps, chromium and molybdenum, which are quite useful as coatings.

We believe that much higher specific energies and powers than those achieved in the studies reported in the literature are possible with sodium/metal chloride cells. One indication of this is the high utilizations reported for $Na/FeCl_2$ cells at low current densities with relatively thick electrodes [7].

The sodium/metal chloride cell appears to have several unique characteristics. These include:

(i) the cell failures are usually in the short-circuit mode, which provides very good battery reliability;

(ii) the reaction of sodium and either $FeCl_2$ or $NiCl_2$ following the fracture of an electrolyte is mild with only a slight temperature rise, a good safety feature;

(iii) high active material densities, and high packing density for the cells result in a high calculated volumetric energy density for the battery and a lightweight, compact, battery insulating case.

To take advantage of these good features, the low power of the present cell design must be circumvented by increasing the electrolyte surface area, which could allow the use of thinner positive electrodes.

One approach to designing high-performance sodium/metal chloride batteries is to design very small cells with small-diameter, thin-walled electrolyte tubes. Calculations at ANL indicate that for this approach the cells would have to be less than 5 A h in capacity for the electric vehicle application, and thus may result in high-cost cell fabrication and complex cell interconnection.

A more promising approach is to develop an electrolyte structure consisting of many long, small-diameter tubes connected to a single header. The sodium could be located either inside or outside the tubes. If the sodium is located inside the tubes, the segregation of the sodium into separate compartments is a good safety feature, and the heat which is developed in the positive electrode on discharge would be more easily transmitted to the wall of the cell from outside the tubes. Whether the sodium is located inside or outside the tubes, each tube may be provided with an individual current collector wire, which can be sealed into the individual tubes. With this design approach, the header may be constructed of a metal that is compatible with the positive electrodes (nickel, for instance). Individual tubes could be sealed into the header with glass. It may be possible to retain some of the flexibility provided by the metal header and permit some movement between the

individual electrolyte tubes, thus avoiding high stresses and cracking that might result from a rigid header structure.

Another approach is to develop a flat-plate electrolyte structure such as that shown in Fig. 7. Individual current collector wires could be sealed into the square pockets, which are probably most appropriate for containing the sodium electrode material.

A comparison of the characteristics of the three types of electrolyte configurations (single large tube, multiple tube, and flat-plate compartmented) is shown in Table 5. A design cell capacity for each of these configurations is shown as the top row of the Table. The 100 A h capacity for the single large tube is typical of that now used in sodium/metal chloride cells. Cell capacities of 200 A h are assumed for a multiple-tube cell and a flat-plate cell having compartment electrolytes. To achieve the assumed capacities for the respective cells, 100 tubes are needed for a multiple tube cell, and 6 electrolyte structures are needed for the flat-plate compartmented cell.

These structures in the assumed sizes provide considerably more electrolyte area than that in the single, large tube cell. The larger electrolyte areas, coupled with the thinner wall thicknesses of the electrolytes, result in much lower voltage losses through the electrolytes, as shown in the Table. The electrolyte dimensions selected for Table 5 are only representative of high surface area designs and could be adjusted to achieve a wide range of power-to-energy ratio.

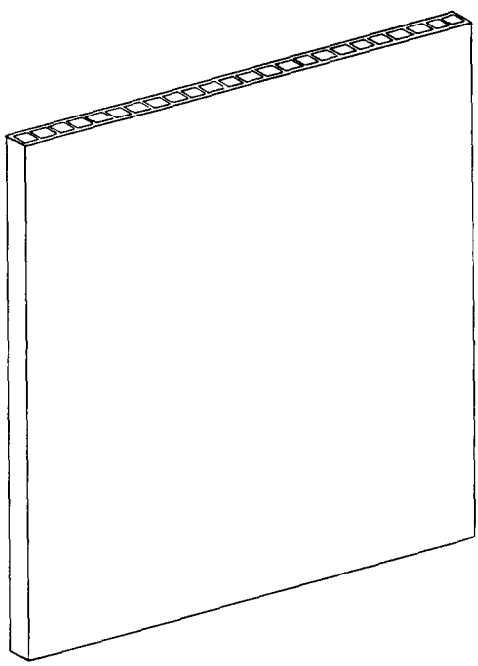

Fig. 7. Proposed flat-plate β''-alumina electrolyte for sodium–metal chloride cell.

TABLE 5

Electrolyte configuration and key cell parameters

	Electrolyte configuration		
	Single large tube	Multiple tube	Flat-plate compartmented
Cell capacity @ 3 h rate (A h)	100	200	200
Electrolyte			
Number of elements	1	100	6
Active length (cm)	30	18	18
Outside dimensions	3.0 cm dia.	0.5 cm dia.	0.4 × 9.0 cm
Wall thickness (mm)	1.5	0.4	0.4
Electrolyte outside area (cm^2)	283	2830	1950
Current density 3 h rate (mA cm^{-2})	118	24	34
Voltage loss @ 1.5 *C* rate at the following resistivities			
6 Ω cm[a] (V)	0.50	0.03	0.04
50 Ω cm (V)	—	0.23	0.31
100 Ω cm (V)	—	0.46	0.62
Positive electrode (central sodium)			
Loading density[b] (A h cm^{-3})	0.25	0.35	0.35
Thickness (mm)	10.5[c]	1.5[d]	2.9[e]

[a] Resistivity of β''-alumina at 250 °C is about 6 Ω cm.
[b] Based on rated capacity of cell.
[c] Radial width of annulus.
[d] Average radial width of annulus (irregular shape).
[e] Half-thickness of flat electrode reacted on both faces.

The voltage losses that develop in the positive electrode are also alleviated by the use of electrolytes having high surface areas. In presently operated sodium/metal chloride cells, the loading density of the positive electrode is frequently about 0.25 A h cm^{-3}. This would result in a radial width for an annular positive electrode of 10.5 mm. At the high current densities required for the small electrolyte area, the voltage loss in this electrode would be very high. At the lower current densities for the high-surface-area designs, higher loading densities should be possible, and a value of 0.35 A h cm^{-3} was assumed in Table 5. For cells with this higher loading density and higher electrolyte surface area, the thicknesses of the positive electrodes are much less than that for the present single tube cell design. Thus, for these cells, the voltage loss in the positive electrode would also be low, even though the fraction of liquid electrolyte in the electrode is lower than that for most of the cells reported to date.

A comparison of the two types of high-surface-area electrolyte configurations considered in Table 5, indicates that each has advantages. The multiple tube configuration probably requires less new development effort for electrolyte fabrication. Also, the tubular electrolytes would be more

easily sealed into a header than the flat-plate electrolytes. The flat-plate compartmented design provides a more advantageous shape for the positive electrode than the multiple tube configuration. For the flat-plate cell, the positive electrodes would consist merely of flat plates pressed against a positive current collector sheet. Provision for the current collector and the loading of the positive electrode in the multiple tube cell would be complex, but clever designs may solve these problems.

Conclusion

Much improvement is possible in the performance of advanced batteries over that which has been achieved thus far. Future efforts in development of both lithium and sodium anode high-temperature batteries are expected to result in batteries that meet the goals that were originally set when development efforts were first initiated: specific energy of about 220 W h kg^{-1}, specific power of 440 W h kg^{-1} and a life of 1000 cycles.

Acknowledgement

The author thanks J. E. Harmon for editorial review of the manuscript. The work reported was funded by the U.S. Department of Energy, Conservation and Renewable Energy, under contract No. W-31-109-ENG-38.

References

1 Z. Tomczuk, B. Tani, N. C. Otto, R. F. Roche and D. R. Vissers, *J. Electrochem. Soc., 129* (1982) 925.
2 T. D. Kaun, *J. Electrochem. Soc., 132* (1985) 3063.
3 T. D. Kaun, T. F. Holifield and W. H. DeLuca, Lithium disulfide cells capable of long cycle life, *Ext. Abstr., 174th ECS Mtg., Chicago, IL, Oct. 1988, Vol. 88-21,* Electrochemical Society, Pennington, NJ, p. 71.
4 T. D. Kaun, T. F. Holifield, M. N. Nigohosian and P. A. Nelson, Development of overcharge tolerance in Li/FeS and $LiFeS_2$ cells, *Ext. Abstr., 174th ECS Meeting, Chicago, IL, Oct. 1988, Vol. 88-21,* Electrochemical Society, Pennington, NJ, p. 67.
5 L. Redey, *Proc. 22nd IECEC Mtg., Philadelphia, PA, Vol. 2,* American Institute of Aeronautics and Astronautics, New York, 1987, p. 1091.
6 J. Molyneux, G. Sands, S. Jackson and I. Witherspoon, *Proc. 22nd IECEC Meeting, Philadelphia, PA, Vol. 2,* American Institute of Aeronautics and Astronautics, New York, 1987, p. 975.
7 R. J. Bones, J. Coetzer, R. C. Galloway and D. A. Teagle, *J. Electrochem. Soc., 134* (1987) 2379.
8 R. M. Dell and R. J. Bones, *Proc. 22nd IECEC Mtg., Philadelphia, PA, Vol. 2,* American Institute of Aeronautics and Astronautics, New York, 1987, p. 1072.
9 A. R. Tilley and R. M. Bull, *Proc. 22nd IECEC Mtg., Philadelphia, PA, Vol. 2,* American Institute of Aeronautics and Astronautics, New York, 1987, p. 1078.
10 J. L. Sudworth, R. C. Galloway and D. S. Dermott, *Electric Vehicles, 73* (Autumn 1987) 14.

11 M. L. Wright and J. L. Sudworth, *Ext. Abstr., 172nd ECS Mtg., Honolulu, HI, Oct. 1987, Vol. 87-7*, Electrochemical Society, Pennington, NJ, p. 149.
12 J. Coetzer, *J. Power Sources, 18* (1986) 377.
13 J. Coetzer and M. J. Nolte, *U.S. Pat. 4,592,969* (1986).
14 R. J. Bones, J. Coetzer, R. C. Galloway and D. A. Teagle, *Ext. Abstr., ECS Mtg., San Diego, CA, Oct. 1986*, Electrochemical Society, Pennington, NJ, p. 1122.
15 J. Coetzer and M. M. Thackeray, *U.S. Pat. 4,288,506* (1986).
16 J. Coetzer, R. C. Galloway, R. J. Bones, D. A. Teagle and P. T. Moseley, *U.S. Pat. 4,546,005* (1985).